Polymer Chemistry

PAPER

Tuneable and degradable thermosets possessing dynamic aliphatic disulfide bonds *via* stereoselective thiol–yne polymerisation†

Daniele Giannantonio, [ID] Arianna Brandolese and Andrew P. Dove [ID] *

The permanent chemical structure that makes thermosets strong and stretchable materials also hinders their reprocessability and leads to their accumulation in the environment. To favour material reprocessability and reuse, polymers have been endowed with dynamic covalent bonds. However, when the dynamic bond is the network-forming bond, a significant trade-off between the robustness of the material and the dynamic behaviour can be encountered. In this study, nucleophilic thiol–yne click polymerisation was used to synthesise different materials possessing tuneable amounts of reversible disulfide bonds, thus achieving diverse thermomechanical properties. Furthermore, by leveraging different catalyst systems, the *cis/trans* conformer ratio on the backbone could be modulated to provide an additional degree of control over the thermomechanical properties. Finally, the presence of dynamic bonds was used as a handle to enable promotion of degradation and material reprocessing.

Introduction

Thermosets are covalently cross-linked materials that find applications in many industries, such as construction,[1] transportation,[2] and aerospace,[3] largely a result of their outstanding strength, extensibility, and solvent resistance. Their cross-linked nature, which is responsible for many of these useful properties, also causes their intractability and limited reprocessability, contributing to environmental concerns.[4] Even when heated at very high temperatures these materials are unable to flow, meaning that they do not melt; hence, the development of reprocessable thermosets constitutes a major goal in polymer science.[5]

Recently, the introduction of dynamic covalent bonds into thermosets established covalent adaptable networks (CANs) as a new class of materials.[6] The dynamic bonds within the materials can break and reform on sufficiently short timescales to allow the polymer chains to undergo molecular rearrangement, thus allowing macroscopic flow in a thermoplastic-like fashion. Parameters such as the nature of the dynamic bonds of choice (*i.e.* associative or dissociative) and the strategy deployed to form the network (step-growth *vs.* chain-growth polymerisation) influence the final architecture and bond distribution.[7,8] Among the different dynamic bonds

available, disulfide bonds have received significant attention because of their widespread presence in biological systems and well characterized dynamic behaviour.[9,10] With a dissociation energy of around 60 kcal mol^{-1}, lower than that of the aliphatic C–C bond of 80–90 kcal mol^{-1}, disulfide bonds provide a good balance between dynamicity and robustness.[11,12]

In light of their efficiency, several thiol-based reactions have been used for the synthesis or functionalisation of polymeric materials.[13] Among these, the use of thiol–ene Michael addition, radical or nucleophilic, arguably represents the most common approach given its simplicity and functional group tolerance.[14–16] Because of the reversibility of the thia-Michael adduct, several CANs built on this reaction have been reported.[17–20] Similarly, the use of activated alkynes allows for the nucleophilic thiol addition across the triple bond.[21–26] Only recently, Du Prez and co-workers reported the use of nucleophilic thiol–yne addition to activated alkynes to obtain CANs with tuneable relaxation rates depending on the electronic of the alkyne of choice.[27] While this work shows that network formation can be achieved through the use of a reversible reaction, only dissociative bonds can be introduced with this approach thus limiting its scope. Moreover, since bifunctional alkynes and thiols are being used, the thiol–yne addition reaction is responsible for the formation of pre-polymers, and only a subsequent thiol–ene addition forms the crosslinked structure.

The use of such a selective reaction represents an advantage because of its efficiency, high yield, and tolerance towards a wide range of functional groups. Additionally, if the presence

School of Chemistry, University of Birmingham, Edgbaston, Birmingham, B15 2TT, UK. E-mail: a.dove@bham.ac.uk

of the dynamic bonds is independent of the polymerisation method, a greater range of reversible moieties can be introduced.[28] Moreover, when a bifunctional alkyne is reacted with a multifunctional thiol (functionalities >2), the prepolymer synthesis step can be bypassed simplifying the network formation. Previous work showed that the ratio of the resulting addition products, the *trans* and *cis* isomers, can be modulated by catalyst and/or solvent selection. In fact, *cis*-enriched products have been synthesised increasing solvent polarity or switching to stronger bases as catalysts.[16,29] This is particularly interesting as backbone *cis/trans* isomerism has been previously used to tailor thermomechanical performances in linear polymers,[30–32] hydrogels,[33] and 3D printable resin,[34] but this concept has not, to date, been applied to CANs. Herein, a bifunctional propiolate possessing an internal dynamic disulfide bond (C_2SS) was here successfully introduced into crosslinked materials by reaction with a three-arm thiol (Fig. 1). The thermomechanical properties of the resulting network were found to change according to the ratio of the monomers and *cis/trans* content. Finally, the presence of dynamic disulfide bonds rendered these materials degradable and reprocessable.

Results and discussion

Network synthesis

To access networks *via* nucleophilic thiol–yne polymerisation, two monomers with activated terminal alkynes (C_2SS and C_6) were synthesised *via* Fisher esterification of commercially available diols with propiolic acid (ESI, Fig. S1–S4†). These monomers were then reacted with a three-arm thiol (trimethylolpropane tris(3-mercaptopropionate) – 3-AT) in different ratios in the presence of an organocatalyst (triethylamine

(Et_3N) or 1,8-diazabicyclo[5.4.0]undec-7-ene (DBU)) in chloroform ($CHCl_3$). The mixtures were poured into Teflon beakers; transparent, flexible, and uniform freestanding films were recovered after slow evaporation of the solvent (ESI, Fig. S5†). Residual solvent was removed by heating at 50 °C under vacuum until constant weight was reached. The versatility entailed by the nucleophilic thiol–yne reaction allows the obtainment of diverse networks from a limited pool of monomers by simple tuning of the reaction conditions. To this end, by employing Et_3N as the catalyst, *trans*-rich networks *trans*-$NetC_2SS$, *trans*-$Net(C_2SS-C_6)$, and *trans*-$NetC_6$ with diverse disulfide content were synthesised by varying the ratio between monomers C_2SS and C_6 (100% C_2SS, 1:1: $C_2SS:C_6$, and 100% C_6 respectively) while keeping the stoichiometric ratio between alkyne and thiol groups 1:1. *trans*-$Net(3-AT_{1.5}-C_2SS_1)$ was accessed by reacting monomer C_2SS with 3-AT in equimolar amounts, to have a thiol:alkyne ratio of 1.5:1. Lastly, *cis*-rich networks $NetC_2SS$ and $NetC_6$ (100% C_2SS and 100% C_6 respectively) were accessed by employing DBU as the catalyst of the reaction.[29,30] Consumption of the alkyne bonds following thiol–yne addition was confirmed by Fourier-transform infrared (FTIR) spectroscopy on the free-standing films, confirming the disappearance of the relative stretching bands (Fig. 2A and B). The formation of networks was further confirmed by performing swelling experiments at room temperature in $CHCl_3$. All networks displayed high gel content (>80%) and a swelling ratio above 250% confirming nucleophilic thiol–yne polymerisation as an excellent tool for the synthesis of crosslinked materials (ESI, Table S1†).

Mechanical properties

Dynamic mechanical analysis (DMA) was performed to evaluate the temperature dependences of storage modulus (E') and
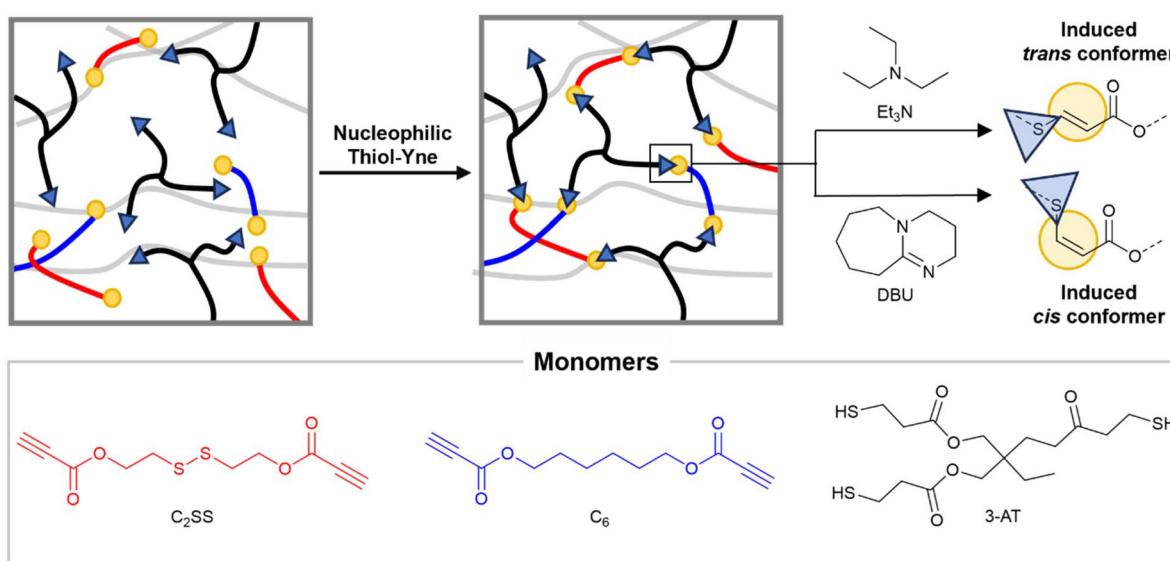

Fig. 1 Scheme representing the network formation and the influence of the catalyst on *cis/trans* isomerism (top) and the monomers used in this work (bottom).
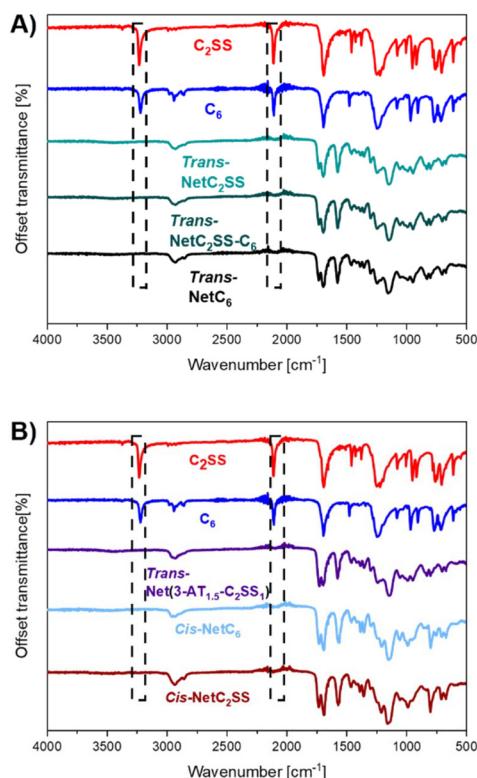
Fig. 2 (A) FTIR spectra showing the disappearance of the alkyne stretching bands in the networks *trans*-NetC$_2$SS, *trans*-Net(C$_2$SS-C$_6$), *trans*-NetC$_6$. (B) FTIR spectra showing the disappearance of the alkyne stretching bands in the networks *trans*-Net(3-AT$_{1.5}$-C$_2$SS$_1$), *cis*-NetC$_2$SS, and *cis*-NetC$_6$.

loss factor (tan δ) of the different networks. The broad and bimodal tan δ curves displayed by the 1 : 1 thiol : alkyne ratio networks suggest that the networks possess a non-homogeneous structure, however, no drop in modulus was recorded (Fig. 3A) which suggests that all materials showed excellent dimensional stability in the temperature range tested (−80 °C to 130 °C). Notably, *trans*-NetC$_2$SS did not display any loss in modulus even at temperatures as high as 180 °C (ESI, Fig. S6†). The absence of a significant drop in modulus above T_g, indicative of a gel-to-sol transition and typically found in dissociative CANs, suggests that these materials behave in an associative "vitrimer-like" fashion.[35,36] The same behaviour has been observed in many CANs possessing both aliphatic[37–39] and aromatic[40–43] disulfide bonds. Nonetheless, a significant decrease in stress could be observed for *trans*-NetC$_2$SS, when stress-relaxation experiments at higher strain (10 μm *vs.* 1 μm) were performed at 150 °C (Fig. 3B). Full relaxation, determined as the time corresponding to ~37% of the initial stress value following a Maxwell model,[44] was reached in roughly 18 minutes. This behaviour was attributed to the dissociation of the disulfide bonds, as *trans*-NetC$_6$ modulus remained constant throughout the experiments. The relatively slow dissociation was linked to the aliphatic nature of the disulfide bonds, which

display higher stability when compared to aromatic disulfides.[11] Even so, this relaxation is consistent with other works displaying aliphatic disulfides. For example, Zhang and colleagues reported variable relaxation rates going from 1.5 s (200 °C) to 90 minutes (60 °C) in a system containing aliphatic disulfide and ester bonds.[39] All materials displayed rubbery behaviour above their glass transition temperature (T_g), as the tan δ dropped to 0.

Fig. 3 (A) DMA (−80 to 130 °C, 5 °C min⁻¹, 1 Hz, 1 μm) curves of the networks synthesised *via* nucleophilic thiol–yne polymerisation. (B) Stress relaxation experiments (150 °C, 10 μm, 20 min) performed on *trans*-NetC$_2$SS and *trans*-NetC$_6$ displaying a loss in modulus for *trans*-NetC$_2$SS exclusively. (C) Exemplary stress *vs.* strain curves obtained from uniaxial tensile testing (10 mm min⁻¹, 22 °C) of different networks synthesised in this work.

When compared to *trans*-NetC$_2$SS, *trans*-Net(3-AT$_{1.5}$-C$_2$SS$_1$) displayed a monomodal and narrower tan δ curve, suggesting that a 1.5 : 1 ratio between thiols and alkyne leads to a more homogeneous network. The decreased molecular weight between crosslinking (M_c) (Table 1) and lower swelling ratio (ESI, Fig. S7 and Table S1†) support this hypothesis, however, very few differences regarding M_c were found among the networks, suggesting that these systems are comparable. The limit of the viscoelastic region (LVE) and yield point determined *via* rheology were found to be similar, as shown by amplitude sweeps performed on the high-*trans* networks (ESI, Fig. S8†). Frequency sweeps confirmed the reduced influence of different degrees of crosslinks on shear stress as the networks did not display strong differences (ESI, Fig. S9†). It is important to note that the density of the material was assumed to be 1 g mL^{-1}, and the theory of rubber elasticity showed some limitations with highly crosslinked systems.[45,46] These data suggest that as different monomer C$_2$SS and C$_6$ ratios were explored, the composition may be responsible for the differences regarding mechanical behaviour, however, when more homogeneous network structures are achieved, these differences can be offset. In fact, *trans*-Net(3-AT$_{1.5}$-C$_2$SS$_1$) was able to compete with a fully carbon–carbon based network such as *trans*-NetC$_6$.

cis-Rich networks showed different properties when compared to their *trans*-rich analogous. While *cis*-NetC$_2$SS displayed a slightly higher rubbery storage modulus ($E'_{rubbery}$) than *trans*-NetC$_2$SS, *cis*-NetC$_6$ possessed a lower $E'_{rubbery}$ value when compared to *trans*-NetC$_6$. Taken together, these results suggest that different degrees of *cis*/*trans* isomerisation can alter the modulus of thermosets, but this effect is mediated by composition as well (Table 1).

Further probing of the mechanical properties was performed *via* uniaxial tensile testing on dogbones cut from the cast films (Fig. 3C, Fig. S10–S15† and Table 1). Despite its lower M_c, *trans*-NetC$_2$SS was found to possess a similar Young's modulus (E) and elongation at break (ε) to *trans*-NetC$_6$. *trans*-NetC$_6$ displayed a slightly higher ultimate tensile strength (UTS) (ESI, Fig. S16–S18†), which is likely a result of its higher carbon–carbon bond content.[11,12] To our surprise, *trans*-Net(C$_2$SS-C$_6$) displayed higher UTS and elongation at break than either network formed from a single alkyne

monomer, (ESI, Fig. S16–S18†) demonstrating that subtle changes to the chemical composition can significantly alter mechanical performance of the resultant materials. When compared to *trans*-NetC$_2$SS, *trans*-Net(3-AT$_{1.5}$-C$_2$SS$_1$) displayed higher Young's modulus ($E = 3.4 \pm 0.7$ MPa *vs.* $E = 0.73 \pm 0.17$ MPa, Fig. S16†) and stress at break ($\sigma = 1.3 \pm 0.6$ MPa *vs.* $\sigma = 0.63 \pm 0.06$ MPa, Fig. S17†), but lower elongation ($\varepsilon = 51.2 \pm 25.4\%$ *vs.* $\varepsilon = 94.8 \pm 22.2\%$, Fig. S18†). These results are consistent with the higher crosslinking density associated with *trans*-Net(3-AT$_{1.5}$-C$_2$SS$_1$), which is also corroborated by its lower swelling ratio (ESI, Table S1†).

Both *cis*-rich networks showed enhanced *UTS* than their *trans*-rich counterparts, confirming that stereochemistry can alter the mechanical properties of thermosets. When compared to *trans*-NetC$_2$SS, *cis*-NetC$_2$SS also displayed significantly higher Young's modulus (ESI, Fig. S16†), while *cis*-NetC$_6$ showed higher elongation at break with respect to *trans*-NetC$_6$ (ESI, Fig. S18†). Comparing the two, *cis*-NetC$_2$SS displayed a higher Young's modulus than *cis*-NetC$_6$ (ESI, Fig. S16†), but no statistically significant differences were observed in stress and strain at break when comparing the results *via* an unpaired T test. However, it is noticeable from the stress–strain curves that the strain at break of *cis*-NetC$_6$ is almost double that displayed by *cis*-NetC$_2$SS, suggesting that further evaluation into the presence of architectural defect could lead to more pronounced differences, underlying once again the trade-off between dynamic behaviour and mechanical performances (ESI, Fig. S17 and S18†). These results suggest that increasing *cis*-content leads to materials possessing a higher strain energy density (Table 1). This may be explained by mechanically induced *cis*-to-*trans* isomerisation, which was probed by Radiom and co-workers.[47] The authors described that when *cis*-rich norbornene polymers were stretched *via* atomic force microscopy (AFM), an increase in extension was measured because of the isomerisation of the shorter *cis* linkages into the longer *trans* conformation, which resulted in relaxation of the force. From a material point of view, this event could lead to energy dissipation, thus allowing the material to withstand greater stress. Notably, *trans*-Net(C$_2$SS-C$_6$), *cis*-NetC$_2$SS, and *cis*-NetC$_6$, displayed ultimate tensile strength and elongation comparable to the likes of styrene butadiene rubber (SBR) and ethylene propylene diene monomer (EPDM), two commonly used elastomers.[48]

Table 1 Summary of thermomechanical data of the networks synthesised in this work

Name	T_g [°C][a]	$E'_{rubbery}$ [MPa][b]	M_c [g mol^{-1}]	E [MPa][c]	σ at break (UTS) [MPa]	ε at break [%]	Strain energy density[d] [J m^{-3}]	T_g [°C][e]	$T_{d, 5\%}$ [°C][f]
trans-NetC$_2$SS	7.25	239.7	34.5	0.73 ± 0.17	0.63 ± 0.06	94.8 ± 22.2	0.34 ± 0.12	−7.4	186.2
trans-NetC$_6$	13.2	1314.2	6.39	0.77 ± 0.4	1.35 ± 0.39	72.5 ± 21.9	0.59 ± 0.28	−7.4	337.8
trans-Net(C$_2$SS-C$_6$)	4.33	506.5	16.1	2.03 ± 0.11	2.56 ± 0.15	155.4 ± 12.6	2.2 ± 0.3	−10.4	300.5
trans-Net(3-AT$_{1.5}$-C$_2$SS$_1$)	4.8	1186.4	6.9	3.4 ± 0.7	1.3 ± 0.6	51.2 ± 25.4	0.39 ± 0.31	−14.4	192.2
cis-NetC$_2$SS	13.25	302.4	27.7	2.5 ± 0.4	3.7 ± 1.9	235.7 ± 101.7	4.9 ± 3.7	−3.2	171.8
cis-NetC$_6$	10.5	720.3	11.6	0.93 ± 0.56	5.7 ± 2.5	471.7 ± 121.9	10.7 ± 5.3	1.3	316.3

[a] Determined as the peak of the tan δ curve. [b] Taken as the value associated with T_g + 50 °C. [c] Determined as the slope of the curve at 1% strain. [d] Determined as the area below the stress *vs.* strain curve. [e] Determined as the inflexion point of the second heating cycle of the DSC thermograms. [f] Determined as the temperature associated with a 5% mass loss.

Thermal properties

Thermal stability was investigated *via* thermogravimetric analysis (TGA) (Fig. 4A and ESI, Fig. S19†). The degradation temperature ($T_{d,5\%}$) was recorded as the temperature associated with a 5% mass loss. The difference in disulfide bond content was found to be the main source of variation among samples, as expected by the lower energy associated with it when compared to the carbon–carbon bond.[11,12] Networks *trans*-NetC$_6$ and *cis*-NetC$_6$ displayed a $T_{d,5\%}$ of 337 °C and 315 °C respectively, which is 151 °C and 145 °C higher than the values recorded for *trans*-NetC$_2$SS and *cis*-NetC$_2$SS. *trans*-Net(3-AT$_{1.5}$-C$_2$SS$_1$) displayed $T_{d,5\%}$ analogous to *trans*-NetC$_2$SS, which is not surprising given the same chemical composition. *trans*-Net(C$_2$SS-C$_6$) $T_{d,5\%}$ was in-between the ones of *trans*-NetC$_2$SS and *trans*-NetC$_6$ at 297 °C. Notably, high *trans*-content networks displayed better stability than their high *cis* counterparts, which agrees with the higher stability associated with *trans* linkages (Table 1).

Differential scanning calorimetry (DSC) revealed all the networks to be amorphous as no melting transition was detected (Fig. 4B and ESI, Fig. S20–S25†). While the higher degree of crosslinking is generally associated with an increase in glass transition temperature (T_g), *trans*-NetC$_6$ underwent transition at the same temperature as *trans*-NetC$_2$SS (−7.4 °C). However, when both monomers were used to synthesise *trans*-Net (C$_2$SS-C$_6$) its T_g was recorded 3 °C lower at −10.4 °C. T_g of *trans*-Net(3-AT$_{1.5}$-C$_2$SS$_1$) was determined at −14.7 °C, roughly 7 °C lower than *trans*-NetC$_2$SS. These observations can be rationalised as a result of unreacted thiols within the network acting as chain-ends, thus increasing the free volume of the network. Both high-*cis* networks revealed T_gs higher than their high-*trans* counterparts, confirming that *cis*/*trans* isomerism can also be used to modulate the thermal properties of the thermosets (Table 1).

Degradability and reprocessability

The presence of dynamic disulfide bonds was leveraged to degrade the networks in a simple reductive fashion.[49] *trans*-NetC$_2$SS and *cis*-NetC$_2$SS were successfully degraded after treatment with an equimolar amount of DL-dithiothreitol (DTT) with respect to the disulfide bond content in 60 h at room temperature in dimethylformamide (DMF) (Fig. 5A and B). The disulfide bond content was estimated based on the initial C$_2$SS monomer feed (ESI, eqn (S4)†). Control experiments performed by treating *trans*-NetC$_6$ under the same conditions (DTT in DMF) and *trans*-NetC$_2$SS without DTT did not show a sign of degradation, confirming that degradation is induced by cleavage of the disulfide bonds (ESI, Fig. S26†). Size-exclusion chromatography (SEC) revealed the formation of low molecular weight peaks only for the samples undergoing degradation (Fig. 5C). The reduced species could be isolated *via* solvent extraction and proton nuclear magnetic resonance (^{1}H NMR) spectroscopy was used to confirm the different *cis*/*trans* ratio of the networks by evaluation of the intensity of peaks in the vinyl region (δ = 5.79 ppm, J = 15.2 Hz, *trans* conformation; δ = 5.89 ppm, J = 10.1 Hz, *cis* conformation) (Fig. 5D and ESI, Fig. S27, S28†). The *cis* content was found to be 26% for *trans*-NetC$_2$SS and 50% for *cis*-NetC$_2$SS. However, it is worth noting that temperature can promote *cis*/*trans* isomerisation,[50] meaning that a more accurate evaluation of the influence of annealing on *cis*-content is required to understand the impact of *cis*/*trans* isomerism on thermosets' thermomechanical properties. Finally, high-resolution mass spectroscopy (TOF-HRMS-ES+) revealed a molecular ion peak at 789 Da for both samples, which matches the molecular weight of macromonomers (788 g mol^{-1}) resulting from cleavage of the disulfide bond (ESI, Fig. S29 and S30†).

Finally, reprocessing of these crosslinked materials was demonstrated by heat compression moulding. *trans*-NetC$_2$SS fragments could be moulded into a free-standing film by heat compression moulding at 150 °C for 20 minutes at a pressure of 3000 kg. The same was possible for *trans*-NetC$_6$, albeit the reprocessed films were less structurally stable. This supports the conclusion that the inclusion of disulfide bonds is the primary driving force of the dynamic behaviour of these materials (ESI, Fig. S31†). Neither network displayed the same homogeneity as the virgin analogues, which suggests that the network structure was not perfectly reformed, possibly in light
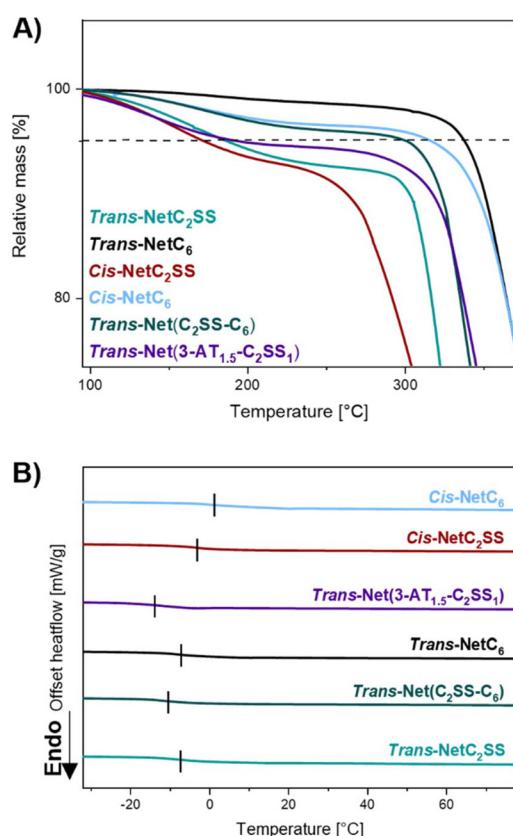
Fig. 4 (A) TGA thermogram (25 °C – 600 °C, N$_2$) of different networks synthesised in this work. $T_{d,5\%}$ decreases with increasing disulfide bond content and higher *cis* content. (B) Zoomed in DSC thermograms (−30 °C to 80 °C, N$_2$) of the second heating cycle of networks synthesised in this work. T_g highlighted by vertical dashes.
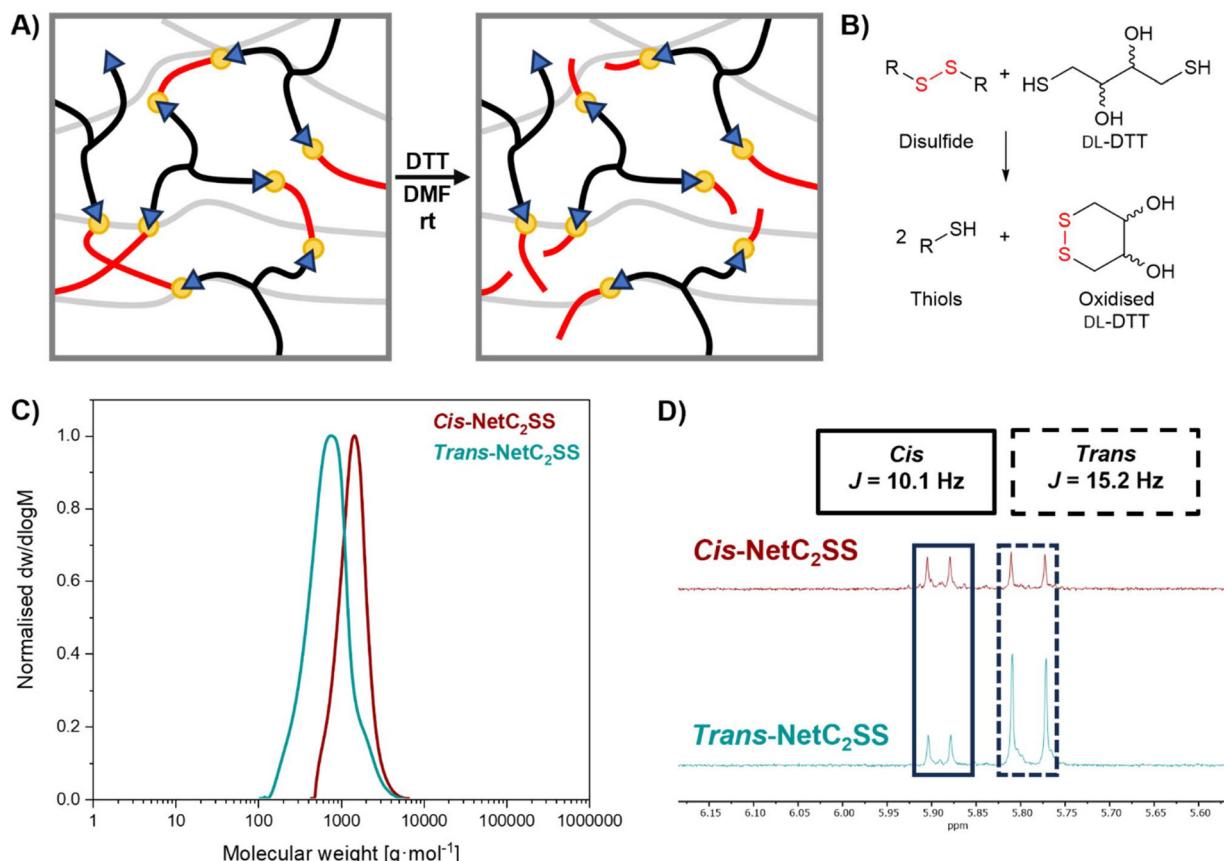
Fig. 5 (A) Schematic representation of DTT degradation of networks synthesised using monomer C_2SS, and formation of the fully reduced species. (B) DTT-mediated reduction of a disulfide bond. (C) SEC (DMF, 5 mM NH_4BF_4, comparison against PMMA standard) of oligomeric species resulting from networks degradation. (D) Zoomed in section of the vinyl region (between 5.60 and 6.15 ppm) of the ^1H NMR spectrum (400 MHz, 300 K, $CDCl_3$) of the products obtained from the degradation of the networks.

of the thermal degradation of the catalysts or of the network itself.[51]

Conclusions

The nucleophilic thiol–yne addition was applied in the synthesis of a library of crosslinked materials in which the thermomechanical properties could be controlled over a broad spectrum, while only using a limited pool of monomers. Notably, this method allows for the simple introduction of dynamic disulfide bonds that endowed the materials with degradability without a considerable loss in performance, compared to their fully aliphatic analogues. While the ratio between thiol and propiolate was found to be crucial in obtaining more homogeneous networks, this method nonetheless allowed for the synthesis of robust materials. Finally, the effect of *cis*/*trans* isomerism on the thermomechanical properties revealed that increasing *cis* content can significantly improve the strain energy density of the network. Lastly, the presence of free thiols resulting from the reduction of disulfides allows us to hypothesise the possibility of establishing a closed-loop recycling life cycle for these materials.

Author contributions

DG: investigation, analysis, manuscript drafting. AB: revision and supervision. APD: conceptualisation, supervision, revision, funding acquisition.

Data availability

The data supporting this article have been included as part of the ESI.†

Conflicts of interest

There are no conflicts to declare.

Acknowledgements

References

1 S. Agarwal and R. K. Gupta, in *Thermosets*, ed. Q. Guo, Elsevier, 2 edn, 2018, pp. 279–302.

2 J. Fan and J. Njuguna, in *Lightweight Composite Structures in Transport*, ed. J. Njuguna, Woodhead Publishing, 2016, pp. 3–34.

3 I. Hamerton and J. Kratz, in *Thermosets*, ed. Q. Guo, Elsevier, 2 edn, 2018, pp. 303–340.

4 R. Geyer, J. R. Jambeck and K. L. Law, *Sci. Adv.*, 2017, **3**, e1700782.

5 D. Rosato and D. Rosato, in *Plastics Engineered Product Design*, ed. D. Rosato and D. Rosato, Elsevier Science, Amsterdam, 2003, pp. 381–438.

6 C. J. Kloxin and C. N. Bowman, *Chem. Soc. Rev.*, 2013, **42**, 7161–7173.

7 C. J. Kloxin, T. F. Scott, B. J. Adzima and C. N. Bowman, *Macromolecules*, 2010, **43**, 2643–2653.

8 P. Chakma and D. Konkolewicz, *Angew. Chem., Int. Ed.*, 2019, **58**, 9682–9695.

9 N. Darby and T. E. Creighton, *Mol. Biotechnol.*, 1997, **7**, 57–77.

10 S. P. Black, J. K. M. Sanders and A. R. Stefankiewicz, *Chem. Soc. Rev.*, 2014, **43**, 1861–1872.

11 Y.-M. Yang, H.-Z. Yu, X.-H. Sun and Z.-M. Dang, *J. Phys. Org. Chem.*, 2016, **29**, 6–13.

12 A. A. Zavitsas, *J. Phys. Chem. A*, 2003, **107**, 897–898.

13 H. Mutlu, E. B. Ceper, X. Li, J. Yang, W. Dong, M. M. Ozmen and P. Theato, *Macromol. Rapid Commun.*, 2019, **40**, 1800650.

14 C. E. Hoyle and C. N. Bowman, *Angew. Chem., Int. Ed.*, 2010, **49**, 1540–1573.

15 A. B. Lowe, *Polym. Chem.*, 2010, **1**, 17–36.

16 J. C. Worch and A. P. Dove, *Acc. Chem. Res.*, 2022, **55**, 2355–2369.

17 B. Zhang, Z. A. Digby, J. A. Flum, P. Chakma, J. M. Saul, J. L. Sparks and D. Konkolewicz, *Macromolecules*, 2016, **49**, 6871–6878.

18 P. Chakma, L. H. Rodrigues Possarle, Z. A. Digby, B. Zhang, J. L. Sparks and D. Konkolewicz, *Polym. Chem.*, 2017, **8**, 6534–6543.

19 N. Kuhl, R. Geitner, R. K. Bose, S. Bode, B. Dietzek, M. Schmitt, J. Popp, S. J. Garcia, S. van der Zwaag, U. S. Schubert and M. D. Hager, *Macromol. Chem. Phys.*, 2016, **217**, 2541–2550.

20 D. Berne, V. Ladmiral, E. Leclerc and S. Caillol, *Polymers*, 2022, **14**, 4457.

21 A. B. Lowe, C. E. Hoyle and C. N. Bowman, *J. Mater. Chem.*, 2010, **20**, 4745.

22 R. Hoogenboom, *Angew. Chem., Int. Ed.*, 2010, **49**, 3415–3417.

23 J. W. Chan, H. Zhou, C. E. Hoyle and A. B. Lowe, *Chem. Mater.*, 2009, **21**, 1579–1585.

24 J. C. Worch, C. J. Stubbs, M. J. Price and A. P. Dove, *Chem. Rev.*, 2021, **121**, 6744–6776.

25 O. Daglar, S. Luleburgaz, E. Baysak, U. S. Gunay, G. Hizal, U. Tunca and H. Durmaz, *Eur. Polym. J.*, 2020, **137**, 109926.

26 B. D. Fairbanks, E. A. Sims, K. S. Anseth and C. N. Bowman, *Macromolecules*, 2010, **43**, 4113–4119.

27 N. Van Herck, D. Maes, K. Unal, M. Guerre, J. M. Winne and F. E. Du Prez, *Angew. Chem., Int. Ed.*, 2020, **59**, 3609–3617.

28 V. Zhang, B. Kang, J. V. Accardo and J. A. Kalow, *J. Am. Chem. Soc.*, 2022, **144**, 22358–22377.

29 V. X. Truong and A. P. Dove, *Angew. Chem., Int. Ed.*, 2013, **52**, 4132–4136.

30 C. A. Bell, J. Yu, I. A. Barker, V. X. Truong, Z. Cao, A. V. Dobrinyin, M. L. Becker and A. P. Dove, *Angew. Chem., Int. Ed.*, 2016, **55**, 13076–13080.

31 C. J. Stubbs, J. C. Worch, H. Prydderch, M. L. Becker and A. P. Dove, *Macromolecules*, 2020, **53**, 174–181.

32 J. C. Worch, A. C. Weems, J. Yu, M. C. Arno, T. R. Wilks, R. T. R. Hucksteep, R. K. O'Reilly, M. L. Becker and A. P. Dove, *Nat. Commun.*, 2020, **11**, 3250.

33 L. J. Macdougall, M. M. Pérez-Madrigal, J. E. Shaw, J. C. Worch, C. Sammon, S. M. Richardson and A. P. Dove, *Angew. Chem., Int. Ed.*, 2021, **60**, 25856–25864.

34 A. L. Khalfa, M. L. Becker and A. P. Dove, *J. Am. Chem. Soc.*, 2021, **143**, 17510–17516.

35 M. Podgórski, B. D. Fairbanks, B. E. Kirkpatrick, M. Mcbride, A. Martinez, A. Dobson, N. J. Bongiardina and C. N. Bowman, *Adv. Mater.*, 2020, **32**, 1906876.

36 J. M. Winne, L. Leibler and F. E. Du Prez, *Polym. Chem.*, 2019, **10**, 6091–6108.

37 W.-Q. Yuan, G.-L. Liu, C. Huang, Y.-D. Li and J.-B. Zeng, *Macromolecules*, 2020, **53**, 9847–9858.

38 D. J. Fortman, R. L. Snyder, D. T. Sheppard and W. R. Dichtel, *ACS Macro Lett.*, 2018, **7**, 1226–1231.

39 M. Chen, L. Zhou, Y. Wu, X. Zhao and Y. Zhang, *ACS Macro Lett.*, 2019, **8**, 255–260.

40 B. Lewis, J. M. Dennis and K. R. Shull, *ACS Appl. Polym. Mater.*, 2023, **5**, 2583–2595.

41 L. Zhou, L. Zhou, R. Chen, G. Chang, K. Zhang and M. Chen, *ACS Appl. Polym. Mater.*, 2023, **5**, 8442–8449.

42 B. Lewis, J. M. Dennis, C. Park and K. R. Shull, *Macromolecules*, 2024, **57**, 7112–7122.

43 A. Ruiz de Luzuriaga, R. Martin, N. Markaide, A. Rekondo, G. Cabañero, J. Rodríguez and I. Odriozola, *Mater. Horiz.*, 2016, **3**, 241–247.

44 B. M. El-Zaatari, J. S. A. Ishibashi and J. A. Kalow, *Polym. Chem.*, 2020, **11**, 5339–5345.

45 C. W. H. Rajawasam, O. J. Dodo, M. A. S. N. Weerasinghe, I. O. Raji, S. V. Wanasinghe, D. Konkolewicz and N. De Alwis Watuthanthrige, *Polym. Chem.*, 2024, **15**, 219–247.

46 T. R. Long, R. M. Elder, E. D. Bain, K. A. Masser, T. W. Sirk, J. H. Yu, D. B. Knorr and J. L. Lenhart, *Soft Matter*, 2018, **14**, 3344–3360.

47 M. Radiom, P. Kong, P. Maroni, M. Schäfer, A. F. M. Kilbinger and M. Borkovec, *Phys. Chem. Chem. Phys.*, 2016, **18**, 31202–31210.

48 T. M. Nair, M. G. Kumaran and G. Unnikrishnan, *J. Appl. Polym. Sci.*, 2004, **93**, 2606–2621.

49 S. N. Mthembu, A. Sharma, F. Albericio and B. G. Torre, *ChemBioChem*, 2020, **21**, 1947–1954.

50 C. Dugave and L. Demange, *Chem. Rev.*, 2003, **103**, 2475–2532.

51 M. A. Alraddadi, V. Chiaradia, C. J. Stubbs, J. C. Worch and A. P. Dove, *Polym. Chem.*, 2021, **12**, 5796–5802.